



U.S. DEPARTMENT OF
ENERGY

Office of
Science

DOE/SC-CM-18-002

**FY 2018 Second Quarter
Performance Metric: Demonstrate
ability to replicate uniform-mesh
high-resolution simulation quality
using local mesh refinement in test-
case or global-ocean configurations**

March 2018

DISCLAIMER

This report was prepared as an account of work sponsored by the U.S. Government. Neither the United States nor any agency thereof, nor any of their employees, makes any warranty, express or implied, or assumes any legal liability or responsibility for the accuracy, completeness, or usefulness of any information, apparatus, product, or process disclosed, or represents that its use would not infringe privately owned rights. Reference herein to any specific commercial product, process, or service by trade name, trademark, manufacturer, or otherwise, does not necessarily constitute or imply its endorsement, recommendation, or favoring by the U.S. Government or any agency thereof. The views and opinions of authors expressed herein do not necessarily state or reflect those of the U.S. Government or any agency thereof.

Contents

1.0 Product Definition	1
2.0 Product Documentation	1
3.0 Results	1
4.0 References	5

Figures

1. Overview of the wind-forced SOMA benchmark model configuration	2
2. Variable-resolution mesh (color scale, in km) for the 4 to 32km SOMA configuration	
3. Mean sea surface height (SSH, m) from (a) uniform, high-resolution (4km) SOMA configuration and (b) from a local mesh refinement (4 to 32km) SOMA configuration.....	3
4. Standard deviation of sea surface height (SSH, m) from (a) the uniform high-resolution (4km) SOMA configuration and (b) the local mesh refinement (4 to 32km) SOMA configuration	4
5. Mean eddy kinetic energy (EKE, m^2s^{-2}) from (a) the uniform high-resolution (4km) SOMA configuration and (b) the local mesh refinement (4 to 32km) SOMA configuration	4

1.0 Product Definition

High-fidelity simulations of the Earth System depend critically on an accurate representation of global ocean currents and their eddies. Earth System Model (ESM) simulations that do not include ocean mesoscale eddy variability have been shown to have numerous biases, including: inaccurate sea surface temperatures (Delworth et al. 2011), weaker meridional heat transport (Kirtman et al. 2012), inaccurate strength and location of western boundary currents (Kirtman et al. 2012, McClean et al. 2011), and poorly represented coastal upwelling (Small et al. 2014). In order to simulate ocean mesoscale eddy variability, an ocean model must resolve the characteristic length scale of mesoscale eddies, referred to as the first Rossby radius of deformation (RRD; Chelton et al. 1998). The quality of eddies produced at different resolutions with respect to the RRD demonstrates the ability of the model to reproduce mesoscale eddy mixing, which is essential for transport of heat, freshwater, and biogeochemical constituents into the global ocean (Dutay et al. 2002, Gnanadesikan et al. 2004, Siegenthaler 1983).

A common way to assess the capability of an ocean model to produce an accurate eddy climate is via the classic eddy-double gyre benchmark (Berloff et al. 2002, Figueroa & Olson 1994, Holland & Lin 1975, Poje & Haller 1999, Straub & Nadiga 2014). The *Simulating Ocean Mesoscale Activity* (SOMA) test case (Wolfram et al. 2015) mimics a strongly eddy-double gyre similar to the North Atlantic Gulf Stream. Here, the SOMA benchmark is used to investigate the ability of local mesh refinement to resolve the eddy climate relative to a uniform, high-resolution-mesh simulation.

A high-fidelity capability for simulating eddies with a variable-resolution ocean is demonstrated in the DOE-ocean model, as validated against the SOMA benchmark

2.0 Product Documentation

The ocean component of the U.S. Department of Energy (DOE)'s Energy Exascale Earth System Model (E3SM) is the *Model for Prediction Across Scale - Ocean* (MPAS-O; Ringler et al. 2013). A new variable-resolution-mesh configuration of MPAS-O has been used for the SOMA test case to understand the capability of local mesh refinement to resolve a strongly eddy ocean climate. SOMA has been configured in MPAS-O at a uniform high resolution of 4km, as in Wolfram et al. (2015), and with variable-resolution using local mesh refinement ranging from 32 to 4km (herein). Here we assess the accuracy of the variable-resolution-mesh approach relative to the uniform, high-resolution approach.

MPAS-O's ability to simulate mesoscale eddy variability using local mesh refinement and to produce a solution with the fidelity of uniform high resolution provides confidence that E3SM can provide improved ocean simulations at lower computational cost. Below, we assess SOMA simulation fidelity both qualitatively (by visual inspection) and quantitatively, using the coefficient of determination r^2 (Crow et al. 1960).

3.0 Results

The SOMA benchmark (Figure 1) is derived from a standard test case of ocean model eddy capabilities forced by a steady zonal wind (Berloff et al. 2002, Figueroa & Olson 1994, Holland & Lin 1975, Poje & Haller 1999, Straub & Nadiga 2014, Wolfram et al. 2015).

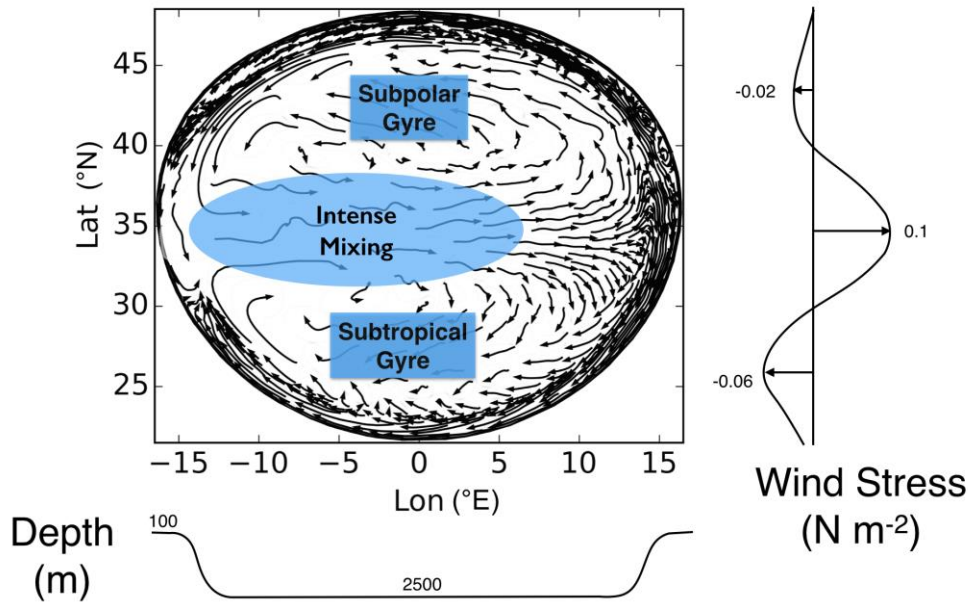


Figure 1. Overview of the wind-forced SOMA benchmark model configuration. Basin bathymetry depth and wind forcing is shown. Average flow vectors in the basin (in black) are shown to highlight the subpolar and subtropical large-scale ocean gyre flows and region of intense mixing in the baroclinic jet between the gyres.

SOMA is initialized from a stratified ocean to approximate the observed pre-existing vertical structure of the ocean. Because eddy production occurs on short time scales, the simulation is spun-up from rest to a quasi-equilibrium state prior to assessment of the eddy climate. Steady zonal wind forcing is applied for five years, to equilibrate the eddy climate, after which the simulation is integrated for another five years while the sea surface height and eddy climatology analysis takes place (Wolfram et al. 2015).

The SOMA benchmark assesses a model's ability to accurately simulate the generation of mesoscale eddies by baroclinic instability, which converts potential energy stored in ocean stratification to kinetic energy via eddies. Baroclinic instability occurs at length scales on the order of the Rossby Radius of Deformation (RRD). Thus, the RRD constrains the size of eddies produced in the SOMA simulation (Vallis 2017). Enhanced resolution is needed to resolve this scale and ensure that eddies are properly simulated.

The characteristic RRD of the idealized mid-latitude SOMA basin is approximately 32km (Wolfram et al. 2015) and the uniform, high-resolution mesh for MPAS-O is approximately 4km, a factor of eight times smaller than the RRD. This high-resolution mesh is well resolved and able to adequately simulate mixing by the eddies (Wolfram et al. 2015). The flow leads to two zonally oriented, counter-rotating, large-scale ocean currents that produce a subpolar gyre, a subtropical gyre, and a baroclinic jet corresponding to a region of enhanced eddy activity (between the gyres at 35° N, as shown in Figure 1).

The local mesh refinement case uses 4km resolution in the western baroclinic jet to resolve the enhanced eddy activity at the interface between the subpolar and subtropical gyres. A lower mesh resolution of 32km is used in the east (Figure 2). The locally refined configuration is expected to fully resolve mesoscale eddy activity in the baroclinic jet and marginally resolve it away from the jet. Here, the

computational benefit of local mesh refinement is a computational savings of approximately 70%, via fewer simulated degrees of freedom.

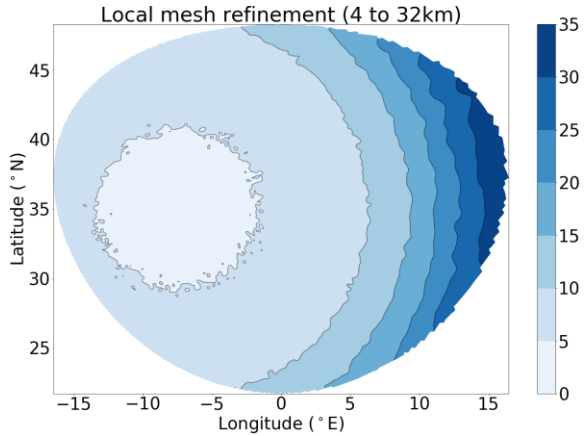


Figure 2. Variable-resolution mesh (color scale, in km) for the 4 to 32km SOMA configuration.

Quantitative assessment of SOMA’s climate when using the variable-resolution mesh is performed using the coefficient of determination r^2 . The comparison is made by linearly interpolating the variable-resolution mesh results onto the uniform, high-resolution mesh.

The MPAS-O SOMA configuration using local mesh refinement (Figure 2) can accurately reproduce the mean sea surface height (SSH) climate of the uniform high-resolution SOMA configuration (Figure 3), which is composed of a subpolar region of decreased sea surface height to the north of 35° N corresponding to the large-scale, counter-clockwise current. Likewise, the large-scale, clockwise current to the south of 35° N is accompanied by a region of elevated mean sea level. The simulation of mean sea surface height with the variable-resolution mesh captures 98% of the variability represented by the uniform-mesh resolution ($r^2 = 0.98$).

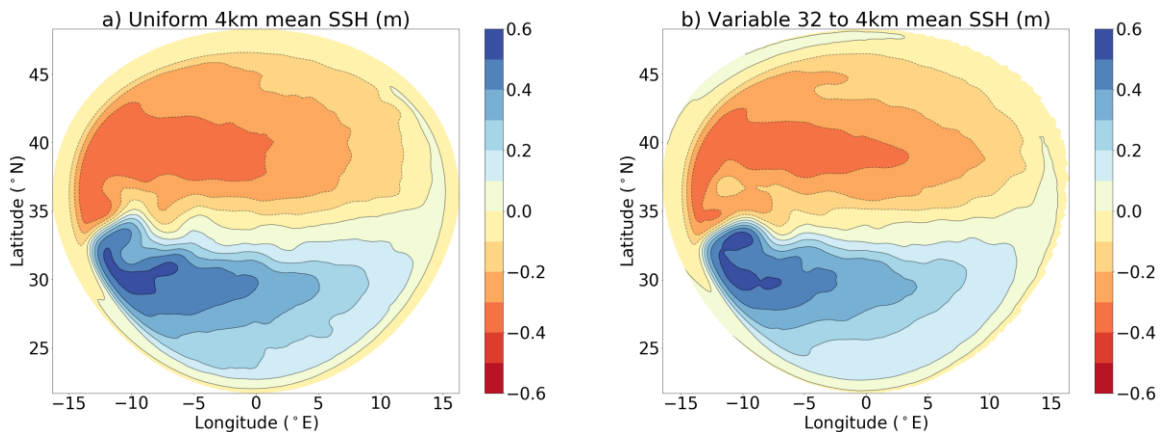


Figure 3. Mean sea surface height (SSH, m) from (a) uniform, high-resolution (4km) SOMA configuration and (b) from a local mesh refinement (4 to 32km) SOMA configuration.

Strong eddy activity occurs at the interface between these large-scale currents and is quantified using the magnitude and structure of the sea surface height standard deviation as well as the eddy kinetic energy. The standard deviation of sea surface height is comparable between the uniform and variable-resolution meshes ($r^2=0.95$, Figure 4).

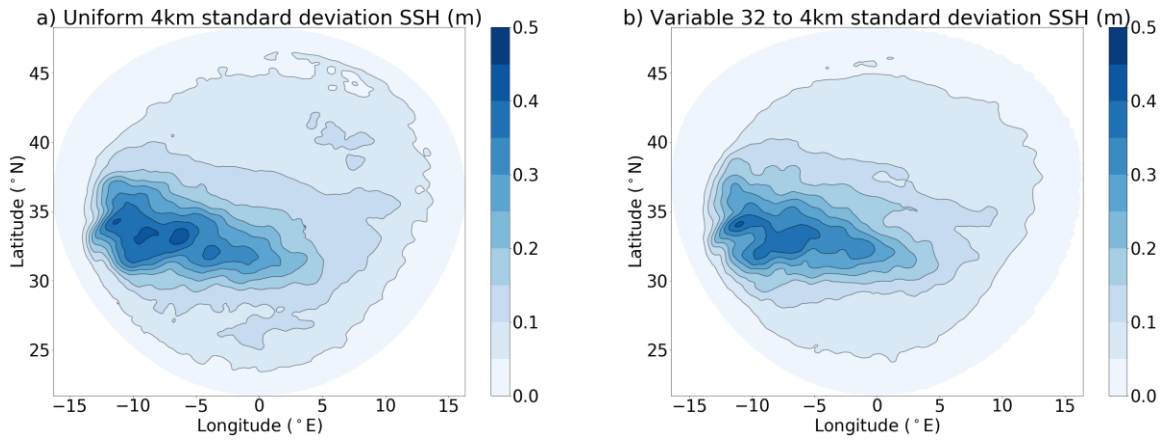


Figure 4. Standard deviation of sea surface height (SSH, m) from (a) the uniform high-resolution (4km) SOMA configuration and (b) the local mesh refinement (4 to 32km) SOMA configuration.

Similar to variability in sea surface height, the eddy kinetic energy is well represented in the locally refined configuration ($r^2=0.95$, Figure 5). The high-quality, variable-resolution solution gives confidence that local mesh refinement is able to adequately reproduce mesoscale eddies.

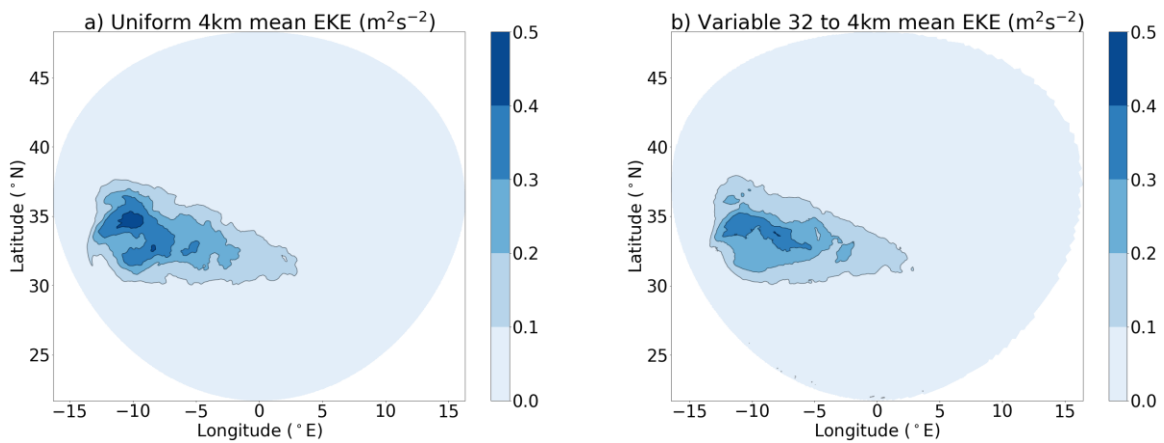


Figure 5. Mean eddy kinetic energy (EKE, m^2s^{-2}) from (a) the uniform high-resolution (4km) SOMA configuration and (b) the local mesh refinement (4 to 32km) SOMA configuration.

In summary, MPAS-O is able to resolve mesoscale activity for the SOMA configuration. The locally refined mesh produces a comparable solution to the uniform, high-resolution mesh, both qualitatively and quantitatively ($r^2 \geq 0.95$ for all standard metrics compared here). Furthermore, a global simulation for the *Coordinated Ocean-ice Reference Experiment* (CORE, Large & Yeager 2004) with local mesh refinement in the North Atlantic was shown to be comparable to a uniform mesh solution (see Ringler et al. 2013, Figures 8-10 therein). These idealistic and realistic simulations demonstrate that simulation quality using a uniform, high-resolution mesh can be replicated with local mesh refinement. This local mesh refinement capability will enable MPAS-O and E3SM to facilitate novel science applications, such as ocean and land-ice interactions, resolution of boundary and coastal currents, and assessment of regional sea level rise and its associated ocean-land interactions.

4.0 References

- Berloff, PS, JC McWilliams, and A Bracco. 2002. "Material Transport in Oceanic Gyres. Part I: Phenomenology." *Journal of Physical Oceanography* 32(3): 764–96, [doi:10.1175/1520-0485\(2002\)032<0764:MTIOGP>2.0.CO;2](https://doi.org/10.1175/1520-0485(2002)032<0764:MTIOGP>2.0.CO;2).
- Chelton, DB, RA deSzoeke, MG Schlax, K El Naggar, and N Siwertz. 1998. "Geographical Variability of the First Baroclinic Rossby Radius of Deformation." *Journal of Physical Oceanography* 28(3): 433–60, [doi:10.1175/1520-0485\(1998\)028<0433:PGVOTFB>2.0.CO;2](https://doi.org/10.1175/1520-0485(1998)028<0433:PGVOTFB>2.0.CO;2).
- Crow, EL, FA Davis, and MW Maxfield. 1960. *Statistics Manual: With Examples Taken from Ordnance Development*. Courier Corporation.
- Delworth, TL, A Rosati, W Anderson, AJ Adcroft, V Balaji, R Bensen, K Dixon, SM Griffies, H-C Lee, RC Pacanowski, GA Vecchi, AT Wittenberg, F Zeng, and R Zhang. 2011. "Simulated Climate and Climate Change in the GFDL CM2.5 High-Resolution Coupled Climate Model." *Journal of Climate*. 25(8): 2755–81, [doi:10.1175/JCLI-D-11-00316.1](https://doi.org/10.1175/JCLI-D-11-00316.1).
- Dutay, J-C, JL Bullister, SC Doney, JC Orr, R Najjar, K Caldeira, JM Campin, H Drange, M Follows, Y Gao, N Gruber, MW Hecht, A Ishida, F Joos, K Lindsay, G Madec, E Maier-Reimer, JC Marshall, and A Yool. 2002. "Evaluation of ocean model ventilation with CFC-11: comparison of 13 global ocean models." *Ocean Modelling*. 4(2): 89–120, [doi:10.1016/1463-5003\(01\)00013-0](https://doi.org/10.1016/1463-5003(01)00013-0).
- Figueroa, HA, and DB Olson. 1994. "Eddy Resolution versus Eddy Diffusion in a Double Gyre GCM. Part I: The Lagrangian and Eulerian Description." *Journal of Physical Oceanography* 24(2): 371–86, [doi:10.1175/1520-0485\(1994\)024<0371:ERVEDI>2.0.CO;2](https://doi.org/10.1175/1520-0485(1994)024<0371:ERVEDI>2.0.CO;2).
- Gnanadesikan, A, JP Dunne, RM Key, K Matsumoto, JL Sarmiento, RD Slater, and PS Swathi. 2004. "Oceanic ventilation and biogeochemical cycling: Understanding the physical mechanisms that produce realistic distributions of tracers and productivity." *Global Biogeochemical Cycles* 18(4): GB4010, [doi:10.1029/2003GB002097](https://doi.org/10.1029/2003GB002097).
- Holland, WR, and LB Lin. 1975. "On the Generation of Mesoscale Eddies and their Contribution to the Oceanic General Circulation. I. A Preliminary Numerical Experiment." *Journal of Physical Oceanography* 5(4): 642–57, [doi:10.1175/1520-0485\(1975\)005<0658:OTGOME>2.0.CO;2](https://doi.org/10.1175/1520-0485(1975)005<0658:OTGOME>2.0.CO;2).
- Kirtman, BP, C Bitz, F Bryan, W Collins, J Dennis, N Hearn, JL Kinter, R Loft, C Rousset, L Siqueira, C Stan, R Tomas, and M Vertenstein. 2012. "Impact of ocean model resolution on CCSM climate simulations." *Climate Dynamics* 39(6): 1303–28, [doi: 10.1007/s00382-012-1500-3](https://doi.org/10.1007/s00382-012-1500-3).
- Large, WG, and SG Yeager. 2004. Diurnal to decadal global forcing for ocean and sea-ice models: The data sets and flux climatologies. NCAR Technical Note, NCAR/TN-460+STR, [doi:10.5065/D6KK98Q6](https://doi.org/10.5065/D6KK98Q6).
- McClellan, JL, DC Bader, FO Bryan, ME Maltrud, JM Dennis, AA Minn, PW Jones, YY Kim, DP Ivanova, M Vertenstein, JS Boyle, RL Jacob, N Norton, A Craig, and PH Worley. 2011. "A prototype two-decade fully-coupled fine-resolution CCSM simulation." *Ocean Modelling*. 39(1-2): 10–30, [doi:10.1016/j.ocemod.2011.02.011](https://doi.org/10.1016/j.ocemod.2011.02.011).

Poje AC, Haller G. 1999. Geometry of Cross-Stream Mixing in a Double-Gyre Ocean Model. *J. Phys. Oceanogr.* 29(8):1649–65, [doi: 10.1175/1520-0485\(1999\)029<1649:GOCSMI>2.0.CO;2](https://doi.org/10.1175/1520-0485(1999)029<1649:GOCSMI>2.0.CO;2)

Ringler, T, M Petersen, RL Higdon, D Jacobsen, PW Jones, and M Maltrud. 2013. "A multi-resolution approach to global ocean modeling." *Ocean Modelling* 69: 211–32, [doi:10.1016/j.ocemod.2013.04.010](https://doi.org/10.1016/j.ocemod.2013.04.010).

Siegenthaler, U. 1983. "Uptake of excess CO₂ by an outcrop-diffusion model of the ocean." *Journal of Geophysical Research – Oceans* 88(C6): 3599–3608, [doi: 10.1029/JC088iC06p03599](https://doi.org/10.1029/JC088iC06p03599).

Small, RJ, RA Tomas, and FO Bryan. 2014. "Storm track response to ocean fronts in a global high-resolution climate model." *Climate Dynamics*. 43(3–4): 805–28, [doi:10.1007/s00382-013-1980-9](https://doi.org/10.1007/s00382-013-1980-9).

Straub, DN, and BT Nadiga. 2014. "Energy Fluxes in the Quasigeostrophic Double Gyre Problem." *Journal of Physical Oceanography* 44(6): 1505–22, [doi:10.1175/JPO-D-13-0216.1](https://doi.org/10.1175/JPO-D-13-0216.1).

Vallis GK. 2017. *Atmospheric and Oceanic Fluid Dynamics*. Cambridge University Press, Cambridge.

Wolfram, PJ, TD Ringler, ME Maltrud, DW Jacobsen, and MR Petersen. 2015. "Diagnosing Isopycnal Diffusivity in an Eddying, Idealized Midlatitude Ocean Basin via Lagrangian, in Situ, Global, High-Performance Particle Tracking (LIGHT)." *Journal of Physical Oceanography* 45(8): 2114–33, [doi:10.1175/JPO-D-14-0260.1](https://doi.org/10.1175/JPO-D-14-0260.1).



U.S. DEPARTMENT OF
ENERGY

Office of Science